

# Dynamical Organization of Directional Tuning in the Primate Premotor and Primary Motor Cortex

YORAM BEN-SHAUL,\* ERAN STARK,\* ITAY ASHER, ROTEM DRORI, ZOLTAN NADASDY,  
AND MOSHE ABELES

Department of Physiology, Hadassah Medical School and the Interdisciplinary Center for Neural Computation,  
The Hebrew University, Jerusalem, Israel 91120

Submitted 14 May 2002; accepted in final form 4 October 2002

**Ben-Shaul, Yoram, Eran Stark, Itay Asher, Rotem Drori, Zoltan Nadasdy, and Moshe Abeles.** Dynamical organization of directional tuning in the primate premotor and primary motor cortex. *J Neurophysiol* 89: 1136–1142, 2003; 10.1152/jn.00364.2002. Although previous studies have shown that activity of neurons in the motor cortex is related to various movement parameters, including the direction of movement, the spatial pattern by which these parameters are represented is still unresolved. The current work was designed to study the pattern of representation of the preferred direction (PD) of hand movement over the cortical surface. By studying pairwise PD differences, and by applying a novel implementation of the circular variance during preparation and movement periods in the context of a center-out task, we demonstrate a nonrandom distribution of PDs over the premotor and motor cortical surface of two monkeys. Our analysis shows that, whereas PDs of units recorded by nonadjacent electrodes are not more similar than expected by chance, PDs of units recorded by adjacent electrodes are. PDs of units recorded by a single electrode display the greatest similarity. Comparison of PD distributions during preparation and movement reveals that PDs of nearby units tend to be more similar during the preparation period. However, even for pairs of units recorded by a single electrode, the mean PD difference is typically large ( $45^\circ$  and  $75^\circ$  during preparation and movement, respectively), so that a strictly modular representation of hand movement direction over the cortical surface is not supported by our data.

## INTRODUCTION

The notion that the motor cortex is organized somatotopically was introduced more than a century ago (Jackson 1958). Since then, somatotopy has served as a framework for numerous studies using various techniques. The emerging picture from studies using microstimulations, extracellular recordings, lesions, and anatomical methods is that the motor cortex is somatotopically organized on a gross level. However, this somatotopy is only a crude approximation of a more realistic description by which representations of specific body regions and muscles intermix and overlap considerably (for a review, see Schieber 2001). Akin to the concept of somatotopy is the idea that *parameters* of movement (and not muscles or body parts per se) are mapped onto the cortical surface (Amirikian and Georgopoulos 1997; Lee et al. 1998). This type of organization is well established in the visual and auditory cortices

with respect to stimulus orientation and tone frequency, respectively (e.g., Hubel and Wiesel 1962; Mountcastle 1978). However, an analogous representation of movement parameters is yet to be demonstrated in the motor cortex.

The activity of motor cortical neurons has been correlated with multiple movement parameters whose relative importance is still under debate (Ashe and Georgopoulos 1994; Cheney and Fetz 1980; Evars 1968; Fu et al. 1995; Kakei et al. 1999; Scott et al. 2001), making it unclear which parameters, if any, are represented over the cortical surface. For instance, Lee et al. (1998), who studied primary motor and parietal cortex neurons during performance of a center-out task, reported that the correlation of the neurons' response functions decreases with interneuronal distance. Another study (Amirikian and Georgopoulos 1997) provided evidence that neurons in the arm area of the motor cortex are arranged in columns of similar and/or opposite preferred hand directions. The present study focuses on one parameter, the preferred direction of hand movement (PD), and studies its representation over the motor cortex [dorsal premotor cortex (PMd) and primary motor cortex (M1)] during two periods in a center-out task. Our analysis is not limited to PDs of units recorded by a single electrode but also to those recorded by a set of adjacent electrodes. In the following, we use the term motor cortex to denote both M1 and PMd.

## METHODS

### Experimental design

Two monkeys (B and T, *Macacca fascicularis*, weight approximately 2.5 kg each) were trained to perform reaching movements from a fixed origin to one of six peripheral targets (circle radius: 3 cm/2.9 cm, monkeys B/T; target radius: 0.5 cm, both monkeys). During task performance, each monkey sat in a primate chair with its left arm restrained and operated a two-joint low-friction manipulandum with the right hand. The medial aspect of the workspace coincided with the monkey's midline and was located approximately 10 cm in front of the monkey at chest level. A cursor indicating the hand position and the targets were projected on a horizontal board at a plane parallel and immediately above that of the manipulandum, so that hand position was mapped directly to cursor position.

The trial sequence is depicted in Fig. 1. As soon as the cursor was

\*Y. Ben-Shaul and E. Stark contributed equally to this work.

Address for reprint requests: Y. Ben-Shaul, Department of Physiology, The Hebrew University, Hadassah Medical School, P.O. Box 12272, Jerusalem, Israel 91120 (E-mail: ybss@md2.huji.ac.il).

The costs of publication of this article were defrayed in part by the payment of page charges. The article must therefore be hereby marked "advertisement" in accordance with 18 U.S.C. Section 1734 solely to indicate this fact.

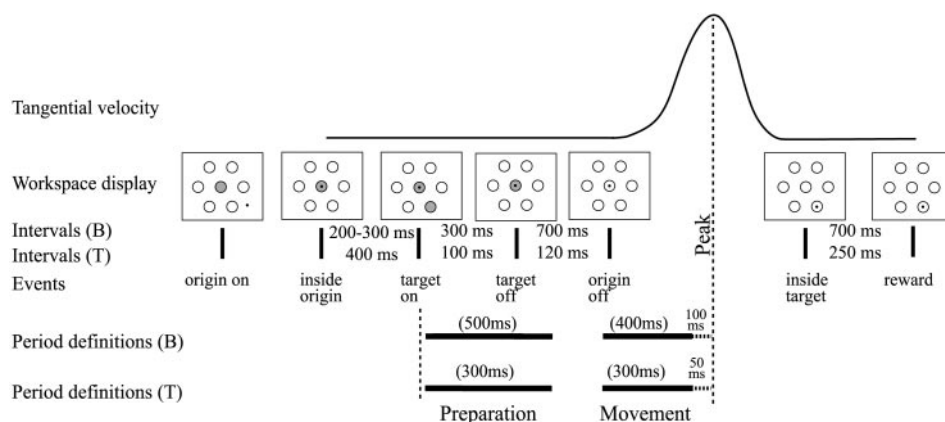


FIG. 1. Behavioral task. *Top trace*: schematic representation of the tangential velocity during execution of a single movement. The visual display that the monkey sees during the trial, key events, and lengths of intervals is depicted below. The origin is the center of the 7-target grid. In reality, the origin was highlighted in red during *origin on* and changed its color to green in *inside origin*. Also, the target (*target on*) was shown in red and changed its color to green when the cursor was positioned in it (*inside target*). The periods used for analysis of the tuning functions of the units are shown as horizontal bars at the bottom. Lengths of intervals (but not their order) differ for the two monkeys and correspondingly so do the period definitions. Note that intervals, period durations, and target sizes are not plotted to scale.

placed within the origin (*inside origin*), the origin changed its color to green. After a delay (200–300 ms for monkey B, 400 ms for monkey T) one of the peripheral targets changed its color to red (*target on*). Following an additional interval (300 ms monkey B, 100 ms monkey T) the red target changed color to gray again (*target off*). The cursor had to be maintained within the origin as long as it remained green. Once the origin changed its color to gray (*origin off*, after 700 ms for monkey B, 120 ms for monkey T), the monkey could move the cursor out of the origin and into the first target (*inside target*). After maintaining the cursor within the target (700 ms for monkey B, 250 ms for monkey T) a juice reward was administered (*reward*). Although the task conditions restricted the monkey to maintain the cursor within the origin until it is dimmed (*origin off*), due to the fixed interval between *trace off* and *origin off*, the time of dimming could be anticipated by the monkeys. Thus motion start sometimes occurred before the origin was dimmed, without the cursor leaving it yet.

### Surgical procedure and data acquisition

Following training, a square recording chamber ( $27 \times 27$  mm) was attached to the skull under deep ketamine–xylazine anesthesia in aseptic conditions. The electrode positioning apparatus (MT, Alpha-Omega Engineering, Nazareth, Israel) included eight glass-coated tungsten electrodes ( $0.2\text{--}1\text{ M}\Omega$  at 1 kHz) guided by a common tube of 1.5-mm ID. Individual electrodes were advanced into the brain using a computer-controlled microdrive (EPS, Alpha-Omega Engineering). The amplified and band-pass-filtered (0.3–6 kHz) signals were fed to a template-matching device (MSD, Alpha-Omega Engineering) to isolate the extracellular activity of 1–3 units per electrode. Spikes (sampled at 1 kHz), behavioral events (1 kHz), and hand position (100 Hz) were logged on a custom-designed data-acquisition system. A quantitative criterion for goodness of spike separation was applied off-line for units recorded by a single electrode. Briefly, based on individual spike shapes, a confusion matrix was derived for each unit pair, and the classification error represented by the matrix was used to select only well-separated units. The majority of recording sites were located in the arm area of the contralateral PMd, and a minority on the convexity of M1, as determined by intracortical microstimulation, passive manipulation of limbs, and examination of penetration sites on the cortical surface (see Fig. 3). On several sessions (monkey B) intramuscular electromyograms (EMG) were recorded from the following proximal and distal arm muscles: extensor carpii ulnaris, flexor carpii ulnaris, biceps brachii, triceps brachii, trapezius, extensor digitorum 45, and palmaris longus. EMG was sampled at 24 kHz and RMS filtered (low-pass 20 Hz). All surgical and animal handling procedures comply with Israeli law and with the guidelines of The Hebrew University.

### Determination of PDs

PDs of individual units were determined using vector summation (see following text) for each unit during two periods within a trial: preparation and movement (Fig. 1). Preparation started with target presentation and ended after 500 ms for monkey B and after 300 ms for monkey T. Movement was defined as the 400-ms period ending 100 ms before attainment of peak velocity (in each trial) for monkey B and the 300-ms period ending 50 ms before attainment of peak velocity for monkey T. The movement period was terminated shortly before attainment of peak velocity because during this interval, both the velocity and the acceleration vector pointed in the same direction. Note that these terms are not entirely appropriate: preparation also includes target presentation, while movement may include reaction time, and does not encompass the entire duration of movement. We nevertheless use this terminology for simplicity's sake. The differences in period definitions between the two monkeys were required due to the differences in the temporal details of their tasks. For each direction, the vector magnitude was taken as the spike count over all movements to that direction within the relevant period. The PD of a unit was defined as the direction of the resultant of the vectors for each of the six directions. Significance of tuning was assessed with bootstrapping (4,000 trials), as described in Crammond and Kalaska (1996). The error in determination of the PD is clearly dependent on the spatial sampling density, which is  $60^\circ$  in our case. Additional critical parameters are the number of trial repetitions, the duration of the interval used for estimating the neuronal response, and the actual (unknown) form of the tuning function. Considering the spatial sampling frequency and the number of trial repetitions (see Table 1) pertaining to our case, for cosine tuning functions our estimate of the PD is essentially unbiased, and its SD is  $<3^\circ$ . For comparison, the corresponding value for sampling at  $45^\circ$  (8 directions) with five trial repetitions is more than  $7^\circ$ .

### Statistical analysis of PD distributions

Throughout this work, we deal primarily with two classes of samples: *electrode samples* and *site samples*. An electrode sample includes the PDs of units recorded by a single electrode (i.e., 1–3 units). A site sample includes units recorded by all (i.e., at most 8) electrodes within a single penetration. Virtually all units belonging to a single electrode sample are confined to a sphere of 100- $\mu\text{m}$  radius (Abeles 1982). Based on the inner diameter of the electrode-guide (1.5 mm), maximal electrode-tip unit distance (100  $\mu\text{m}$ ), and depth measurements of the electrode-positioning system, we estimate that units from a common site sample are confined to a cylinder with a 1.7-mm-diam base and approximately 2-mm height. Note that these distances are upper bounds and not typical values. Distances between units from different site samples are generally much larger, depending on the actual penetration sites on the cortical surface (Fig. 3A).

A variety of standard methods for testing circular data for uniformity exists (cf. Mardia 1972), but these methods can only be applied to samples of at least four observations. Since our data set includes PD samples with as few as two observations, we applied two other approaches: the circular variance test and a direct comparison of pairwise PD differences.

### The circular variance test

The circular variance ( $S_n$ ) of a sample of  $n$  directional observations ( $\theta_j$ ) is given by (Mardia 1972)

$$S_n = 1 - \frac{1}{n} \sqrt{\left(\sum_{j=1}^n \cos \theta_j\right)^2 + \left(\sum_{j=1}^n \sin \theta_j\right)^2}$$

Spread out observations tend to cancel each other, driving their circular variance toward one, whereas, for clustered observations, the circular variance approaches zero. We denote the probability of obtaining a circular variance equal to or smaller than the observed value  $S_n$ , assuming directions are distributed uniformly over the circle, by  $F_u(S_n)$ . The function  $F_u(S_n)$  was derived numerically using a Monte-Carlo procedure with 20,000 iterations for each sample size ( $n$ ) separately. Representative samples, their circular variances, and the corresponding  $F_u(S_n)$  are shown in Fig. 2. As can be seen in Fig. 2B, the form of the distribution depends on sample size. For large samples, the distribution converges to the one used in Rayleigh's test (Mardia 1972).

To increase the power of our statistical tests, we considered the sets of electrode samples and site samples. Specifically, we characterize the clustering tendency of a set of site samples and electrode samples by the geometric mean of the  $F_u(S_n)$  over all samples within that set, and denote it by  $GM_{sites}$  and  $GM_{elec}$ , respectively. The geometric mean is defined as  $(\prod F_u)^{1/N}$ , where the multiplication is over the  $F_u$  of each of the  $N$  samples in the set. Intuitively, the geometric mean can be regarded as the probability of obtaining the observed set of samples, normalized by the number of samples in the set. To test for clustering within the electrode samples set, we compared the observed  $GM_{elec}$  to its distribution under the hypothesis that PDs are independently drawn from the entire cortical population. This probability was estimated with 6,000 bootstrapped values of  $GM_{elec}$ , where each was obtained by randomly allocating PDs from the entire cortical sample to electrodes. Due to the confounding effect of electrode samples on site samples containing them, testing for site sample sets is slightly more complex. Therefore, to obtain the observed statistic  $GM_{sites}$ , we diluted site samples, leaving only one unit per electrode. The units eliminated from the sample were chosen such that the circular variance of the diluted sample was maximized. For example, if a site contained PDs from two electrodes, one with a single unit whose PD is  $0^\circ$  and another with a pair of units with PDs  $0^\circ$  and  $90^\circ$ , we eliminated the  $0^\circ$  unit from the second electrode and obtained a site sample of two individual units with PDs of  $0^\circ$  and  $90^\circ$ . For the 6,000 bootstrapping trials, we also diluted site samples (leaving one unit per electrode), but here the eliminated units were chosen randomly on each bootstrapping trial. Overall, our procedure for testing site sample uniformity is conservative, as the dilution imposed on site samples for deriving the observed  $GM_{sites}$  maximizes this statistic. The bootstrapping procedure was conducted separately for the data from each monkey and each period.

### Comparison of PD differences

Pairwise PD differences (Fig. 2) were calculated between pairs of units conforming to each of the following three categories:

- 1) The set of pairs of units from the same electrode samples.
- 2) The set of pairs of units from the same site samples, but not from the same electrode samples.
- 3) The set of pairs of units recorded at different sites.

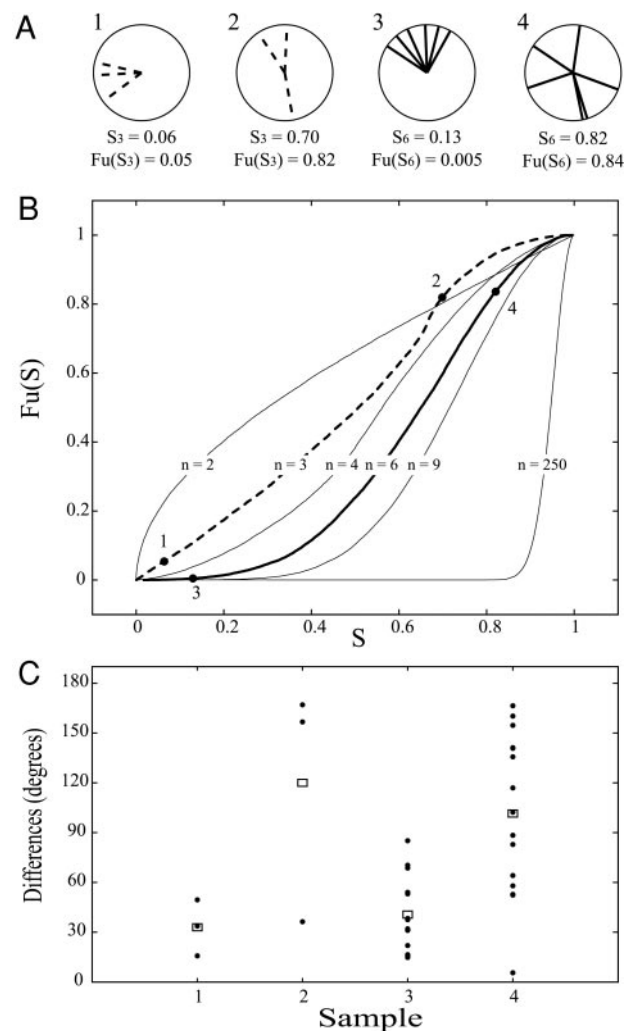


FIG. 2. Illustration of the statistical methods. A: samples 1 and 2 are from single electrodes, each containing 3 preferred directions (PDs). Samples 3 and 4 are from single sites, each with 6 PDs. B: cumulative circular variance distributions for various sample sizes. Each trace shows the cumulative distribution function (CDF) of the circular variance  $F_u(S)$  for a sample size of  $n$ . CDFs corresponding to samples in A are shown in broken/bold lines. Clustered samples (1 and 3) receive low values of  $F_u(S)$  whereas spread-out samples (2 and 4) are associated with higher values. C: pairwise differences in each sample. Mean PD differences are indicated by rectangles. Clustered samples are associated with small differences while spread-out samples are associated with larger differences.

Comparison of the PD difference distributions between these categories was performed with a one-tailed two-sample Kolmogorov-Smirnov test.

## RESULTS

Means and SDs of key task interval durations as well as path lengths are shown in Table 1. Inspection of these intervals with respect to the duration of the preparation and movement periods indicates that, for monkey T, these periods were often overlapping. For example, preparation often contained the initial portion of motion. In addition, although the periods were clearly nonoverlapping for monkey B, the movement period also contained some preparatory activity. Thus the names given to each of the periods indicate the predominant, but not the exclusive type of activity associated with each. Visual

TABLE 1. Key task interval durations and path lengths

Monkey	Target on to Peak Velocity, ms	Target on to Start Motion, ms	Origin off to Start Motion, ms	Start Motion to Peak Velocity, ms	Path Length, cm
B	1348 ± 143	1103 ± 141	82 ± 142	245 ± 43	2.56 ± 0.26
T	551 ± 72	270 ± 50	44 ± 50	281 ± 54	2.42 ± 0.3

Values are means ± SD.  $n = 2412$ , monkey B;  $n = 2510$ , monkey T. To calculate these values, all individual trajectories (in each of the 6 directions) were pooled for each monkey separately. Start motions of each trial is defined as time when tangential velocity reaches 15% of the peak value.

inspection of monkey behavior (on-line and off-line on video tape) revealed that hand transport is largely due to arm and to a lesser extent to wrist motion. This observation was also supported by EMGs recorded during motions (monkey B), showing that, although wrist musculature is active on certain directions, proximal muscles are dominant. Although eye movements were not recorded, microstimulation sessions did not reveal any eye movement-related activity. A qualitative evaluation of neuronal activity while looking at spontaneous eye movements also did not reveal any eye-movement-related activity.

In our database we only include units whose significance level for tuning was 1% or smaller and whose classification error with respect to other units recorded by the same electrode was smaller than 2.5%. Table 2 lists the total number of units, the total number of sites (and specifically the number of sites with <4, between 4 and 9, and >9 units), and the number of electrodes with one, two, or three units for both the preparation and the movement periods. An electrode from which more than one unit was recorded constitutes an electrode sample. For example, during preparation for monkey B, the 11 pairs and the single triplet amount to 12 electrode samples (Table 2). The table also shows the number of trials (for each direction) during which units included in the database were recorded from.

Figure 3A shows the basic data for our analysis. In each panel of Fig. 3A (see Fig. 3C for a magnified view), the PD of each unit is indicated by one line, emanating from a dot corresponding to the center of the recording site (that is, the horizontal location into which the center of the guide tube was aimed). Units within a given site, recorded by a single electrode, are shown using the same color and line-type (continuous vs. dashed). As the figure shows, the number of tuned units is larger during movement than during preparation. Note also that, for monkey B, a rostral/caudal gradient whereby tuned units are generally more rostral is evident during preparation. That absence of such a gradient for monkey T during preparation may be due to the fact that, for this monkey, the preparation period typically contained movement-related activity as well. During movement for both monkeys, tuned units

are located in both rostral and caudal regions of the cortical surface from which penetrations were made.

The entire PD sample was tested for uniformity separately for each monkey within each period. As shown in the four panels of Fig. 3B, PDs from both monkeys seem to be uniformly distributed. This observation is also verified by statistical testing for uniformity using Rao's test of equal spacing, since the null hypothesis of equal spacing could not be rejected for any of the cases ( $P > 0.2$  for all cases). Nevertheless, in our subsequent analyses, no assumptions regarding the uniformity of the distributions are made.

#### Circular variance test

Figure 4A shows histograms of all electrode and site samples'  $F_u(S_n)$  for each monkey in the two periods. Comparison of the observed  $GM_{elec}$  to its bootstrapped distribution showed that the likelihood of obtaining the observed or a smaller value of  $GM_{elec}$  was smaller than 1% for both monkeys during preparation and smaller than 5% during movement. We therefore reject the hypothesis of random allocation of PDs to electrode samples for both monkeys during both periods. The null hypothesis of random allocation to sites from the entire cortical sample could also be rejected for site samples, during preparation for monkey T at the 1% level, but not for monkey B (however, the  $P$  value for monkey B comes close to significance at 0.065, and the test is conservative). For the movement period, this hypothesis was rejected at the 5 and 1% level for monkeys B and T, respectively. The results of the circular variance test for each monkey, period, and sample type (electrode or site) appears in the legends of the appropriate panels in Fig. 4A.

#### Comparison of PD differences

Pairwise PD differences were calculated from the data for each monkey separately and then pooled for each category across both monkeys. The hypothesis that PD differences in corresponding categories and periods over both monkeys are derived from the same distribution (6 comparisons, 3 categories × 2 periods, Kolmogorov–Smirnov two-sample test) could

TABLE 2. Units, their allocation into site and electrode samples, electrode samples, and trials per direction for preparation and movement periods

Period/Monkey	Units	Sites	Units Per Site			Units Per Electrode			Electrode Samples	Trials Per Direction		
			1–3	4–9	>9	1	2	3		Median	Minimum	Maximum
Preparation/B	106	29	17	11	1	81	11	1	12	40	8	105
Movement/B	226	39	10	25	4	136	33	8	41	38	6	85
Preparation/T	52	17	11	6	0	41	4	1	5	79	35	158
Movement/T	63	17	11	5	1	44	8	1	9	83	35	158

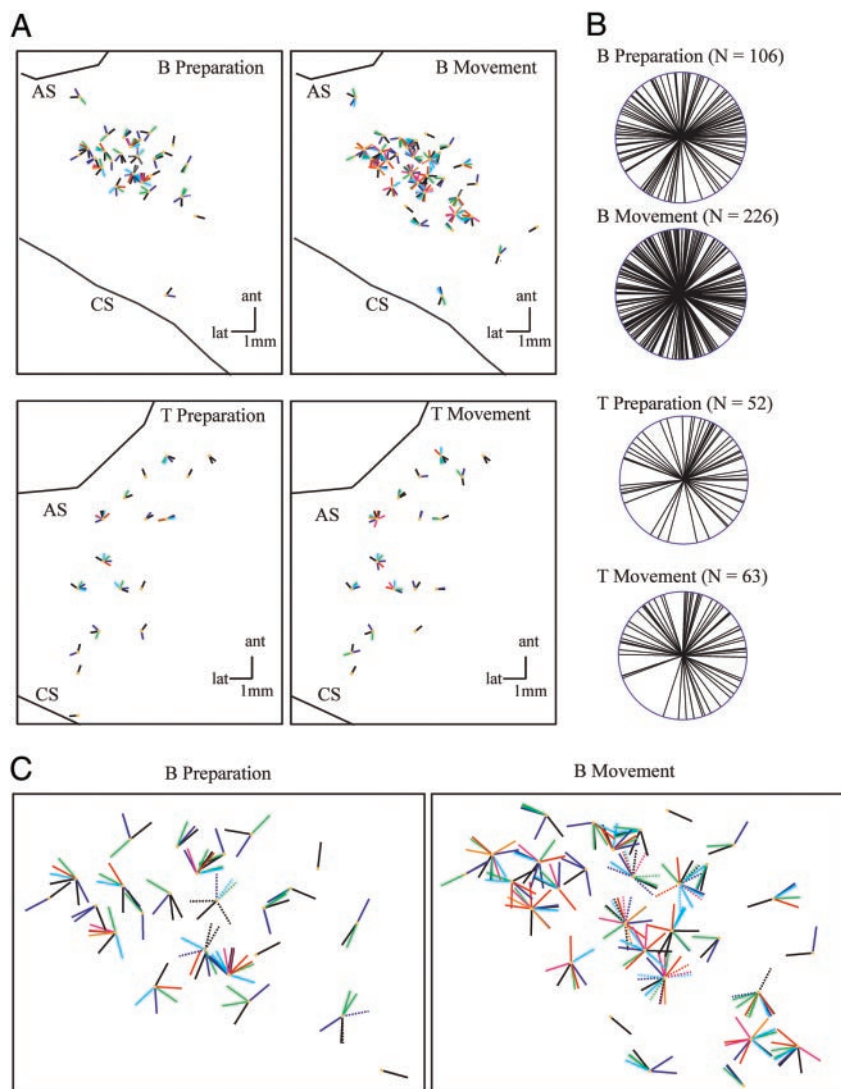


FIG. 3. Basic data. *A*: penetration sites and PDs of all units in the database, plotted for each monkey and each period separately. Preferred direction of each unit is depicted by the direction of a line, starting at the location of the penetration site (yellow dot). Horizontal distances between units recorded from a common site are not shown. All units recorded by a single electrode are shown as lines of the same color and line-type (dashed or continuous) emanating from a common location. Therefore sites including dashed lines correspond to cases when two penetrations were made from the same site (but in sessions spaced a few days apart). *B*, monkey B; T, monkey T; AS, arcuate sulcus; CS, central sulcus. *B*: polar plot of entire PD sample of each monkey within each period. Statistical testing showed that for all four samples, the hypothesis of equal spacing could not be rejected (Rao's equal spacing test). *C*: magnified view of the densest penetration region during preparation and movement for monkey B.

not be rejected ( $P > 0.1$ ) except for one case. The exception was the different sites category during the movement period. Since this category was expected to contain a heterogeneous set of PD differences for each monkey and since the intersite distances were not identical for both monkeys (Fig. 3), we also pooled across this category for subsequent analyses.

The two panels in Fig. 4B show the empirical cumulative distributions of PD differences within each category during preparation and movement. Each trace corresponds to the distribution within one category (dark line: same electrode, intermediate line: same site, light line: different sites). During both periods, PD differences from the same electrodes exhibited smaller values than those from same sites, which in turn were smaller than those from different sites. The results of the pairwise comparison of PD distributions across categories using a Kolmogorov-Smirnov test is also shown in the figure by lines pointing at each pair of traces. The only comparison yielding a nonsignificant difference is between same electrode and same site samples during movement. Despite the lack of a significant difference, the cumulative distribution plots and the insets in Fig. 4B indicate that differences are indeed the smallest within the same electrode sample.

The insets in each of the panels in Fig. 4B show the means and

SEs of PD differences in each category (preparation:  $44.3 \pm 9.5^\circ$ ,  $76.0 \pm 3.0^\circ$ , and  $90.0 \pm 0.6^\circ$  for the same electrode, same site, and different site categories respectively; movement:  $76.4 \pm 6.6^\circ$ ,  $84.9 \pm 2.0^\circ$ , and  $89.7 \pm 0.3^\circ$  for the corresponding categories; sample sizes: preparation: 21, 270, and 6,600 comparisons for the same electrode, same site, and different site categories; movement: 68, 762, and 26,548 for the corresponding categories). Comparison across the same categories under the two periods shows that same electrode and same site pairwise PD differences are different at the 5% level, while different site PD differences are not significantly different (Kolmogorov-Smirnov, two-sample test). In this comparison, overlapping, but not identical sets of units are involved during each of the epochs, since the units fulfilling the selection criteria are not the same during both periods. However, the same results regarding the differences across the two periods are obtained also when the set of units considered is the intersection of the units from both periods.

#### *Dependence on horizontal intersite distances and on vertical electrode-tip distances*

In categorizing into three groups, we lumped together pairs of units from different sites into a single category, ignoring the

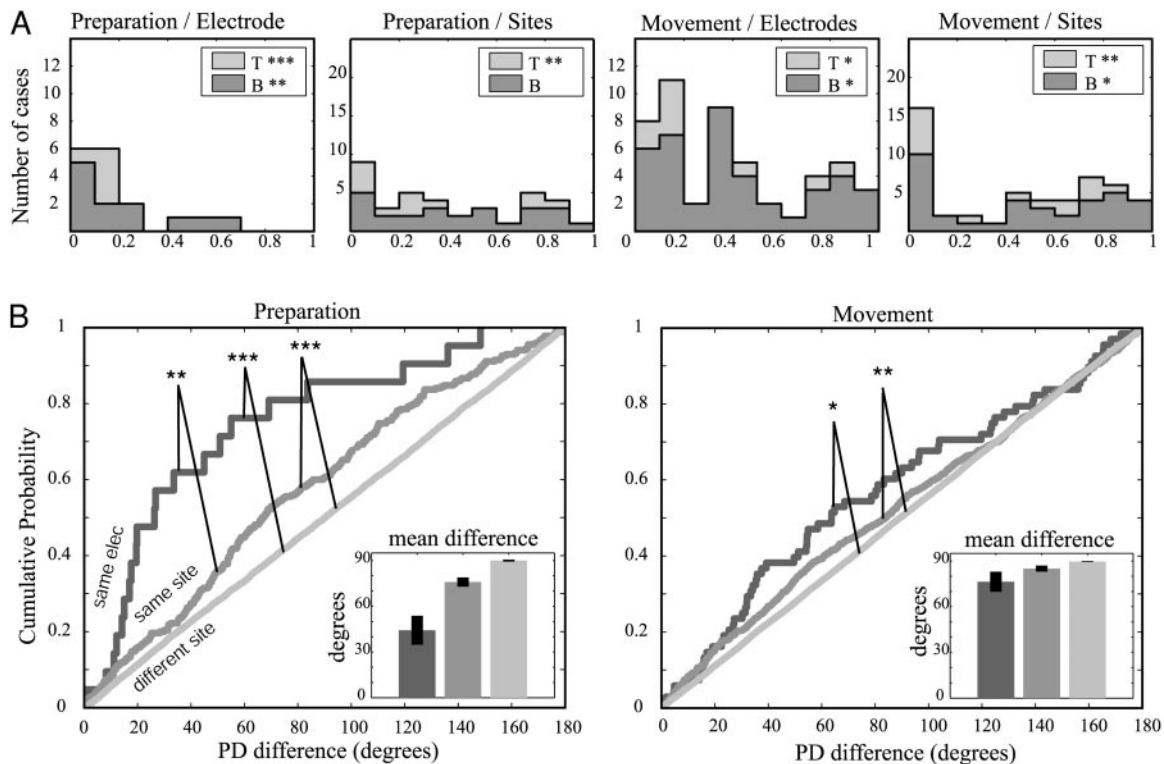


FIG. 4. Results. *A*: analysis of electrode and site samples using the circular variance test. Each panel shows histograms of  $F_{ij}(S)$  of site or electrode samples for both monkeys in one period. Bars in dark and light gray correspond to monkeys B and T, respectively. The total height of each column is therefore the total count for both monkeys. The legend for each bar also indicates the significance of the geometric mean (GM) of the respective sample (\* $P < 0.05$ ; \*\* $P < 0.01$ ; \*\*\* $P < 0.001$ ). Note that the significance is not determined by the histograms, but rather by the position of the geometric mean of all  $F_{ij}(S)$  of the samples in the set, relative to those obtained from the resampled trials. *B*: analysis of pairwise PD differences. Each panel shows results for pooled data from both monkeys within one period. Each of the 3 traces in a panel shows the empirical cumulative distribution of PD differences within one category. Result of the comparison between each pair of categories is also indicated. *Insets*: means and SE of PD differences within each category. Number of comparisons for each category: preparation: 21, 270, and 6,600 for the same electrode, same site, and different site categories; movement: 68, 762, and 26,548 for the corresponding categories.

actual distances between these sites. Therefore, in addition to the analyses reported above, we examined various measures of similarity between PDs as a continuous function of intersite distance. These included distances of site PD distributions (using Wheeler's two-sample uniform-scores test, Mardia 1972) as well as pairwise PD differences. In these and related analyses, we did not find any consistent dependence of PD similarity on distance over the cortical surface.

In addition, we studied whether the vertical distance between electrode tips within a common site was correlated with the PD differences of the units recorded by them. Here, as well, no significant difference could be found between PD differences of units recorded by (vertically) nearby electrode tips versus those recorded by more distantly located tips.

## DISCUSSION

This study reports an analysis of PDs of cortical neurons during preparation and movement periods in the context of a center-out task. The analysis indicates that, during both periods, PDs of single units are not randomly distributed over the cortical surface. In general, PDs of neighboring units (recorded by a single electrode) are more similar than those of units recorded by different electrodes from a single site. PDs of units recorded on a single site are more similar than those of units

recorded from different sites, which in turn are not more similar than expected by chance. The magnitude of these similarities is not identical for the two periods. During preparation, the PD differences of units recorded by the same electrode or within the same site are markedly smaller than those of units recorded during the movement period. Visual inspection of the pairwise PD differences (Fig. 4B) shows that this effect is more pronounced for the same electrode category, though both for this category and for the same site category, PD differences are significantly different compared across both periods ( $P < 0.05$ ). PD differences within the different site category are not significantly different during the two periods. Considering the actual values of the differences, even within the same electrode category (i.e., for neighboring units), the PD differences are often substantial, assuming a mean value of approximately  $45^\circ$  during preparation and  $75^\circ$  during movement. We did not observe the peaks in PD difference for  $0^\circ$  and  $180^\circ$  or  $120^\circ$  (see Fig. 4B), as reported by Amirikian and Georgopoulos (1997). Thus our findings argue against a strict columnar organization of PDs in M1 and in PMd, which would imply a narrower distribution of PDs within electrode samples and correspondingly a peak around PD differences of  $0^\circ$ . However, our results are consistent with the abovementioned work in that they demonstrate a nonrandom distribution of PDs. In addition, such a nonrandom distribution of PDs within

local sites is in line with the observation that local field potentials in the primary motor cortex are tuned for direction of motion (Donchin et al. 2001; E Vaadia, personal communication).

Various analyses conducted in an attempt to uncover a more detailed relationship between PD similarities and intersite distances failed to reveal any consistent dependency. Additionally, though our data do not allow for determination of the cortical layer recorded from, we did study PD differences as a function of electrode-tip distance and found no consistent relationship between it and PD differences.

In a minority of cases, electrodes from a single site may have been more distant (horizontally) than electrodes from neighboring sites. An additional source of measurement error is due to the curved surface of the cortex. Although we aimed the guide tube at a normal angle to the cortical surface, the brain's curvature implies that the horizontal distance between penetration sites, as measured by the electrode-positioning apparatus, is not translated accurately onto the cortical surface. The fact that no detailed pattern of PD representation on the cortical surface emerged may be partially accounted for by these types of measurement error. However, even with error-free and sufficiently dense measurements, a suitable metric is required to reveal any underlying pattern. Consideration of PD distributions as a function of distance alone (as done here), when the underlying organization is complex, would fail to reveal the details of the pattern. Although we made an effort to minimize any spike-sorting errors using the classification criterion, any remaining errors are likely to render observed PDs of neighboring units *more* similar one to another. Thus the values presented here can be considered as a *lower* bound estimate of PD differences between next neighbors.

Here we have focused on a single extrinsic kinematic parameter, the direction of hand movement. However, it may well be that an intrinsic (e.g., joint related) and/or dynamic parameter (e.g., force) is more appropriate (Mussa-Ivaldi 1988). Indeed, finding that a given parameter is represented on the cortical surface in some well-defined pattern would support the idea that the motor cortex utilizes the coordinate frame defined by that parameter for motion control. Since extrinsic and intrinsic coordinate frames are generally coupled (Ajemian et al. 2000), implying that specific parameters may be associated with a number of covariates, our results could also reflect a nonrandom distribution of PDs within some other frame of reference, or with respect to another parameter, and therefore cannot be used to infer the coordinate system that is most appropriate for describing motor cortical organization.

What accounts for the period-related change in PDs of nearby units? One option is that the change is due to the inclusion of additional units (those showing reliable tuning) during movement. However, when considering the set of units obtained by intersecting the sets from preparation and movement, same electrode pairwise PD differences tend to diverge from each other during movement compared with preparation. It has already been shown that PDs change dynamically during the course of a motor task (Mason et al. 1998). Comparison of PD differences of units from same electrode samples (most comprising only a pair of units) between preparation and movement suggests a particular pattern for this dynamic reor-

ganization of PDs where nearby units tend to "decorrelate" or diverge with respect to their preferred direction.

Although two discrete temporal intervals were analyzed here, we do not suggest that the dynamical changes in the pattern of PDs and their differences is discrete. This comment is especially valid as preparation and movement do not represent purely preparatory or movement-related activity and are even overlapping for monkey T. More research is required to elucidate how PD distributions change continuously over time and whether spatial distributions of additional characteristics of the tuning functions (e.g., width and amplitude) are subject to similar dynamic modulations.

We thank H. Bergman, Y. Prut, and S. Hocherman for critical reading of the manuscript and helpful suggestions, E. Singer for the English proofreading, and V. Sharkansky for invaluable technical help. We are grateful to the anonymous reviewers for suggestions and comments, which have substantially influenced the revised form of the manuscript.

This study was supported in part by an Israeli Science Foundation grant.

## REFERENCES

- Abeles M.** *Local Cortical Circuits*. Berlin: Springer-Verlag, 1982.
- Ajemian R, Bullock D, and Grossberg S.** Kinematic coordinates in which motor cortical cells encode movement direction. *J Neurophysiol* 84: 2191–2203, 2000.
- Amirikian B and Georgopoulos AP.** Motor cortical organization of preferred directions. *Soc Neurosci Abstr* 23: 607.6, 1997.
- Ashe J and Georgopoulos AP.** Movement parameters and neural activity in motor cortex and area 5. *Cereb Cortex* 6: 590–600, 1994.
- Cheney PD and Fetz EE.** Functional classes of primate corticomotoneuronal cells and their relation to active force. *J Neurophysiol* 44: 773–791, 1980.
- Crammond DF and Kalaska JF.** Differential relation of discharge in primary motor and premotor cortex to movement posture during reaching movements. *Exp Brain Res* 108: 45–61, 1996.
- Donchin O, Gribova A, Steinberg O, Bergman H, Cardoso de Oliveira S, and Vaadia E.** Local field potentials related to bimanual movements in the primary and supplementary motor cortices. *Exp Brain Res* 140: 46–55, 2001.
- Evarts EV.** Relation of pyramidal tract activity to force exerted during voluntary movement. *J Neurophysiol* 31: 14–27, 1968.
- Fu QG, Flament D, Coltz JD, and Ebner TJ.** Temporal encoding of movement kinematics in the discharge of primary motor and premotor neurons. *J Neurophysiol* 73: 836–854, 1995.
- Hubel D and Wiesel T.** Receptive fields, binocular interaction and functional architecture in the cat's visual cortex. *J Physiol (Lond)* 160: 106–154, 1962.
- Jackson JH.** On the anatomical and physiological localization of movements in the brain. In: *Selected Writings of John Hughlings Jackson: On Epilepsy and Epileptiform Convulsions*, edited by J. Taylor, G. Holmes, and F. M. R. Walshe. New York: Basic Books, 1958, vol. 1, p. 37–76.
- Kakei S, Hoffmann DS, and Strick PL.** Muscle and movement representations in the primary motor cortex. *Science* 285: 2136–2139, 1999.
- Lee D, Port N, Kruse W, and Georgopoulos AP.** Variability and correlated noise in the discharge of neurons in motor and parietal areas of the primate cortex. *J Neurosci* 18: 1161–1170, 1998.
- Mardia KV.** *Statistics of Directional Data*. London: Academic, 1972.
- Mason CR, Johnson MTV, Fu QG, Gomez JE, and Ebner TJ.** Temporal profile of the directional tuning of the discharge of dorsal premotor cortical cells. *Neuroreport* 9: 989–995, 1998.
- Moutcastle VB.** An organizing principle for cerebral function: the unit module and the distributed system. In: *The Mindful Brain*, edited by G. M. Edelman and V. B. Moutcastle. Boston: MIT Press, 1978, p. 7–50.
- Mussa-Ivaldi FA.** Do neurons in the motor cortex encode movement direction? An alternative hypothesis. *Neurosci Lett* 91: 106–111, 1988.
- Schieber MH.** Constraints on somatotopic organization in the primary motor cortex. *J Neurophysiol* 86: 2125–2143, 2001.
- Scott SH, Gribble PL, Graham KM, and Cabel DW.** Dissociation between hand motion and population vectors from neural activity in motor cortex. *Nature* 413: 161–165, 2001.